OXFORD

Cerebral Cortex, 2022, 1–12
https://doi.org/10.1093/cercor/bhac198
Original Article

Graph-theoretical insights into the effects of aging on the speech production network

Jana Schill[1*], Kristina Simonyan[2,3], Maximilian Corsten[1], Christian Mathys[4,5,6], Christiane Thiel[5,7], Karsten Witt[1,5]

[1]Department of Neurology, School of Medicine and Health Sciences, University of Oldenburg, Heiligengeisthöfe 4, 26121 Oldenburg, Germany,
[2]Department of Otolaryngology – Head & Neck Surgery, Harvard Medical School, Boston, 243 Charles Street, Boston, MA 02114, United States,
[3]Department of Otolaryngology – Head & Neck Surgery, Massachusetts Eye and Ear, 243 Charles Street, Boston, MA 02114, United States,
[4]Institute of Radiology and Neuroradiology, Evangelisches Krankenhaus, University of Oldenburg, Steinweg 13-17, 26122 Oldenburg, Germany,
[5]Research Center Neurosensory Science, University of Oldenburg, Carl-von-Ossietzky-Straβe 9, 26129 Oldenburg, Germany,
[6]Department of Diagnostic and Interventional Radiology, University of Düsseldorf, Moorenstraβe 5, 40225 Düsseldorf, Germany,
[7]Department of Psychology, School of Medicine and Health Sciences, University of Oldenburg, Ammerländer Heerstraβe 114–118, 26129 Oldenburg, Germany
*Corresponding author: Heiligengeisthöfe 4, 26121 Oldenburg, Germany. Email: jana.schill@uni-oldenburg.de

Speech production relies on the interplay of different brain regions. Healthy aging leads to complex changes in speech processing and production. Here, we investigated how the whole-brain functional connectivity of healthy elderly individuals differs from that of young individuals. In total, 23 young (aged 24.6 ± 2.2 years) and 23 elderly (aged 64.1 ± 6.5 years) individuals performed a picture naming task during functional magnetic resonance imaging. We determined whole-brain functional connectivity matrices and used them to compute group averaged speech production networks. By including an emotionally neutral and an emotionally charged condition in the task, we characterized the speech production network during normal and emotionally challenged processing. Our data suggest that the speech production network of elderly healthy individuals is as efficient as that of young participants, but that it is more functionally segregated and more modularized. By determining key network regions, we showed that although complex network changes take place during healthy aging, the most important network regions remain stable. Furthermore, emotional distraction had a larger influence on the young group's network than on the elderly's. We demonstrated that, from the neural network perspective, elderly individuals have a higher capacity for emotion regulation based on their age-related network re-organization.

Key words: healthy aging; speech production network; functional magnetic resonance imaging; network analysis; emotional distraction.

Introduction

Studies have shown that speech processing and speech production change in healthy aging (Mortensen et al. 2006; Abrams and Farrell 2011; Sörös et al. 2011). Although there are different theories to explain the emergence of these alterations (MacKay and Burke 1990; MacDonald and Christiansen 2002; Dagerman et al. 2006; Lustig et al. 2007), the brain changes underlying altered speech in healthy aging are not fully understood.

It is well known that speech production requires the interplay of different brain regions (Blank et al. 2002; Heim 2005; Sörös et al. 2006; Hickok and Poeppel 2007; Price 2012; Fuertinger et al. 2015). Graph-theoretical network analysis (Bullmore and Sporns 2009) provides a comprehensive framework for the investigation of how different brain regions build large-scale functional networks. Two aspects of network function, namely network segregation and integration, are commonly used to characterize a network and to highlight differences between networks. Network segregation describes how functionally clustered information processing is within the network, whereas network integration refers to how well information from segregated areas can be integrated, that is, jointly processed (Friston 2011). Studies on RSNs have shown network integration to remain stable even in later life stages (Song et al. 2014; Geerligs et al. 2015; Varangis et al. 2019). Network segregation has been somewhat controversial, with some studies reporting an increase during healthy aging (Sala-Llonch et al. 2014; Shah et al. 2018), whereas others found a decrease (Chan et al. 2014; Song et al. 2014). Furthermore, Meunier et al. (2009) have shown that although network modularity does not differ between age groups, network communication patterns change with age.

Although there is an abundance of network studies on resting state brain function, network literature on speech processing is scarce. A study by Simonyan and Fuertinger (2015) on whole-brain connectivity illustrated that the speech production network (SPN) differs from the whole-brain resting state network (RSN), in that it recruits more regions (i.e. the IPL and the cerebellum) than the whole-brain RSN, is characterized by a functionally more dominant left hemisphere and is more integrated as well as more segregated. However, this study did not compare age groups, so that it remains unclear whether aging effects found in the whole-brain RSN are also present in the SPN.

Received: March 3, 2022. **Revised:** April 29, 2022. **Accepted:** April 30, 2022

Therefore, we aim to compare the whole-brain speech production network between healthy agers and young individuals. We employ different graph-theoretical analysis methods, looking at network metrics and network communication patterns using a picture naming paradigm to assess active network metrics. We expect changes in metrics and hub distribution similar to those reported in the RSN mentioned previously (Meunier et al. 2009; Sala-Llonch et al. 2014; Song et al. 2014; Geerligs et al. 2015; Shah et al. 2018; Varangis et al. 2019). However, as healthy elderly individuals are commonly able to communicate in a sufficient way, we hypothesize that there might be key areas in the brain, namely those that play a key role in the SPN, whose communicative contributions to the network are robust against aging effects. To investigate this, we introduce the notion of network pillars, which carry the communicative load of the network. We then assess how aging affects the presence and distribution of these network pillars.

In addition, we included emotional primes into our study paradigm. Similar to its influence on speech processing, healthy aging has been shown to affect emotional processing. The positivity effect proposed by Carstensen and Mikels (2005) describes the phenomenon that elderly individuals are more sensitive to positive information and tend to neglect negative information. Furthermore, the elderly seem to have an increased capacity for emotion regulation (Eldesouky and English 2018). In young adults, emotional priming has been shown to interfere with cognitive functions (Dolcos and McCarthy 2006; Gupta and Raymond 2012; Hur et al. 2017). We hypothesize that healthy elderly individuals might be more robust against emotional priming in terms of behavioral outcome as well as concerning changes in brain activity.

It has been suggested that resting state connectivity shapes task-based connectivity (Di et al. 2013; Cole et al. 2014, 2016). We therefore expect aging-related changes in the whole-brain SPN to reflect those reported for resting state connectivity. Based on RSN research, we hypothesize that network integration of the SPN will remain stable during healthy aging, but network segregation will increase (Sala-Llonch et al. 2014; Song et al. 2014; Geerligs et al. 2015; Shah et al. 2018; Varangis et al. 2019). Furthermore, we expect that emotional priming will increase network segregation and decrease network integration in the young group, as has been shown previously by Zhang et al. (2015). However, due to changes in emotional processing described previously, we hypothesize the influence of affective priming on the elderly's network to be less pronounced. Lastly, we hypothesize that regions, which play a key role in the SPN will remain stable during aging and after emotional distraction.

Methods

Participants

Twenty-five young healthy volunteers and 25 elderly healthy volunteers were recruited for this study. All participants were right-handed native German speakers. Exclusion criteria were neurological and/or psychiatric diseases, articulation disorders, and regular intake of psychoactive drugs (medical or recreational). Handedness was determined with help of the Edinburgh Handedness Inventory (Veale 2014). To rule out the presence of depressive symptoms, the Beck Depression Inventory II (Beck et al. 1996) was used.

Four participants had to be excluded from the study. One named the primes in addition to the objects and therefore solved a different task, 1 participant exhibited too much head movement during scanning and 2 participants presented with an abnormal mean connectivity strength in both conditions as determined by an outlier analysis using Tukey's fences (Tukey 1977). Therefore, 23 young healthy volunteers and 23 old healthy volunteers were included in the analysis (Table 1). Groups were matched in gender and years of education. As was to be expected, elderly individuals exhibited more head motion (average as well as maximum displacement) than younger individuals. However, head movement was censored during preprocessing to account for this (see Functional network construction).

All participants gave their written informed consent. This study was approved by the local ethics committee and was conducted in accordance with the Declaration of Helsinki.

Experimental paradigm

During the functional magnetic resonance imaging (fMRI) scans, participants underwent an overt picture naming task. In 2 runs, participants were shown a total of 60 every-day inanimate objects taken from the Bank of Standardized Stimuli (Brodeur et al. 2014), which they were supposed to name correctly (30 per run, Fig. 1). Preceding each picture was a presentation of a facial prime showing either a neutral (neutral condition) or a disgusted (disgusted condition) expression. Primes were obtained from the Radboud Faces Database (Langner et al. 2010). Fifteen male and 15 female faces were chosen. Faces were pseudo-randomly matched with objects such that each object was once preceded by the neutral and once by the disgusted version of the same face. Each face appeared once per run (but with 2 different expressions). Each object appeared twice, either in the first or in the second run. Primes were shown for 300 ms, immediately followed by 1,000 ms of stimulus presentation. During the inter-stimulus interval of 8,700 ms a white background was shown. Overt naming task can cause movement artefacts in MRI scans. This was accounted for in later processing steps (see Functional network construction). After the fMRI scans, participants solved the same task in an acoustic chamber, where their answers were recorded for further analysis. The number of correct responses was obtained in both settings (magnetic resonance imaging, MRI and acoustic chamber). Performance in the scanner was 99.1% in the young group and 98.9%

Table 1. Participant characteristics.

	Young	Elderly	P
Age	24.6 ± 2.2	64.1 ± 6.5	< 0.001
Gender (f/m)	13/10	12/ 11	0.77
Years of education	17.6 ± 2.2	17.7 ± 4.0	0.98
Montreal Cognitive Assessment	29.0 ± 1.2	28.4 ± 1.3	0.11
Average head motion (relative)	0.078 ± 0.018	0.144 ± 0.039	< 0.001

Note: Statistical significance was determined using unpaired *t*-tests, except for gender, for which significance was determined with a Qui^2 test.

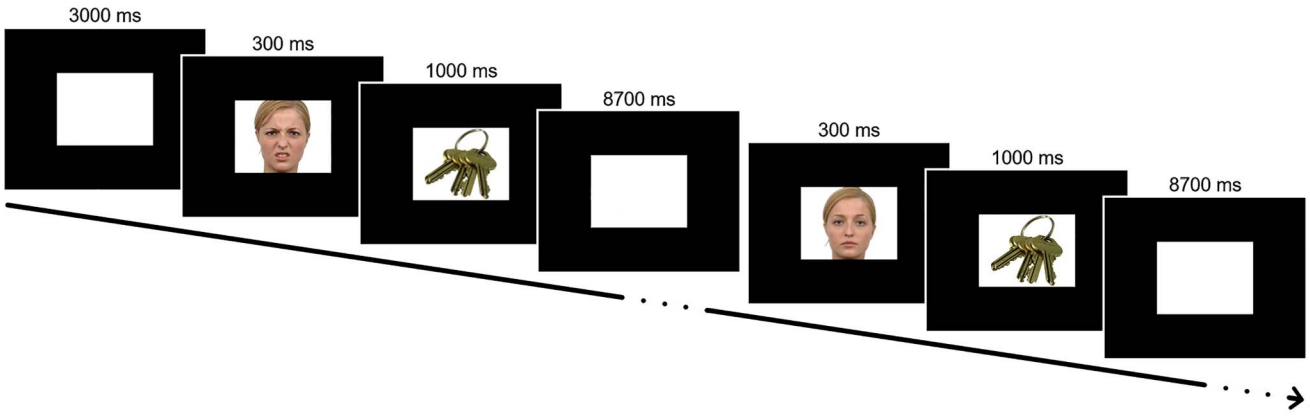

Fig. 1. Experimental paradigm: facial primes were presented for 300 ms, immediately followed by a 1,000-ms presentation of the object to be named. Then a white background image was shown for 8,700 ms. Each object appeared twice, once preceded by a neutral and once by a disgusted expression of the same face.

in the elderly group. As performance in the acoustic chamber was 99.4% for the young group and 98.3% in the elderly group, the tasks were deemed comparable. Only correct answers were included in the MRI analysis. Participants were asked to score all facial primes on a scale from 1 (negative emotional expression) to 9 (positive emotional expression). These emotional scores were used to assess whether there were age differences in perceived emotional valence of the facial stimuli.

Behavioral analysis

Audio recordings were analyzed to assess differences in speech onset due to emotional distraction. Chronset (Roux et al. 2017) was used to automatically determine latencies for all recordings. The recordings of 3 participants had to be manually noise corrected before being fed into Chronset, as noise levels were too high to allow for the algorithm to successfully detect speech onset. Emotional scores of the facial primes were averaged for each condition (neutral and disgusted) and then compared between groups. Both speech onset and emotional scores analysis was done by a mixed analysis of variance (ANOVA), where group served as a between subject factor and emotion (neutral and disgusted) served as a within subject factor ($P < 0.5$).

Image acquisition

A 3T whole-body MRI scanner (Siemens Magnetom Prisma, Siemens Healthineers, Erlangen, Germany) with a 64-channel head coil was used to acquire structural and functional scans. Stimuli were presented using Cogent 2000 developed by the Cogent 2000 team at the Leopold Muller Functional Imaging Laboratory and the Institute of Cognitive Neuroscience and Cogent Graphics developed by John Romaya at the LON at the Wellcome Department of Imaging Neuroscience.

A whole-brain echo planar imaging (EPI) sequence with the following parameters was used to obtain the functional scans: 310 volumes, 36 slices, time repetition (TR) = 2 s, time echo (TE) = 30 ms, slice thickness = 3 mm, field of view (FOV) = 192 mm × 192 mm, flip angle = 75°, and voxel size = 3 × 3 × 3 mm^3.

Structural images were obtained as 3D T1-weighted scans using a magnetization prepared rapid gradient-echo (MPRAGE) sequence with the following parameters: 1 volume, 224 slices, TR = 2 s, TE = 2.07 ms, TI = 952 ms, slice thickness = 0.75 mm, FOV = 240 mm × 240 mm, flip angle = 9°, and voxel size = 0.75 × 0.75 × 0.75 mm^3.

Task activation analysis

In order to better understand what kind of brain activation was elicited during our paradigm, we ran a general linear model (GLM) task activation analysis. This can be found in the Supplementary Material.

Functional network construction

After skull stripping the structural images with ANTs software (Avants et al. 2011) preprocessing for the graph-theoretical analysis was done using in-house AFNI (Cox 1996) code created by running afni_proc.py. First, the first 4 volumes of the functional scans were removed to assure signal stability. All EPI images were despiked using

default settings, temporally aligned to the beginning of the TR using a Fourier interpolation, spatially aligned to the first volume and normalized to the Talairach–Tournoux space (nonlinear transformation). In addition, scans were spatially smoothed using a 4-mm full width at half maximum Gaussian kernel. Finally, the voxel time series were normalized to their percent signal change, meaning that they were scaled such that their mean was set to 100. This allows for better comparison between scans. TRs with motion artefacts above 0.5 mm were censored during the following analysis by removing them from the data set without interpolation. This affected a maximum of 6% of TRs per participant. One participant presenting with extensive head motion, leading to the exclusion of >20% of TRs, was excluded from the analysis. The final preprocessed images were then used for network construction.

Brain regions of interest (ROIs) were defined using masks obtained from the cytoarchitectonic probability maps and macrolabel atlas (Eickhoff et al. 2005; Fuertinger et al. 2015). A total of 212 ROIs (142 cortical, 36 subcortical, and 34 cerebellar) were included in the analysis.

For every ROI in every participant a time series was computed by averaging the signals of the fMRI task of every voxel within the ROI. Separate time series were obtained for each condition, by only including trials of that condition. For each trial (consisting of 300-ms facial prime, 1,000-ms object presentation, and 8,700-ms blank screen), we included 4 TRs in the time series, starting with the first TR after object presentation. With the such constructed time series, each participant's condition-specific connection matrix was constructed by calculating normalized mutual information (NMI) coefficients as a measure of pairwise regional interactions. NMI coefficients were chosen over Pearson's correlation because they come with the inherent advantage of being non-negative, while preserving the nonzero structure of the Pearson's correlation (Fuertinger and Simonyan 2017). To calculate NMI coefficients, the classical mutual information (Cover and Thomas 2012) was divided by the geometric mean of the associated Shannon entropies (Shannon 1948). Therefore, the NMI is a statistical dependence measure taking values from 0 (statistical independence) to 1 (mutual statistical dependence).

For both conditions separately, participants' connectivity matrices were group-averaged. The groups' connectivity matrices were then used to create weighted undirected graphs in which the ROIs were nodes and the NMI coefficients were edge weights. Participants whose connectivity matrices had an abnormal mean connectivity strength according to Tukey's fences (Tukey 1977) were excluded from the respective group matrices.

Network density was calculated by dividing the number of edges present in the graph (i.e. the number of nonzero NMI coefficients) by the number of possible connections. As densely connected networks can show random graph characteristics (Humphries et al. 2006; Lynall et al. 2010), percolation thresholding was applied to the group-averaged networks to ensure that connections included in the further analysis were meaningful to the task and not resulting from noise and artefacts. Percolation thresholding was performed as described by Bordier et al. (2017). Their approach was shown to be an appropriate thresholding method for settings where differences in network density might be data inherent (Bordier et al. 2017).

Network construction scripts were written in Python 3.7 (using open source libraries NumPy (Oliphant 2015), SciPy (Virtanen et al. 2020), and Matplotlib (Hunter 2007)).

Graph-theoretical network analysis

The 2 groups were compared separately for each condition (neutral and disgusted) and for each group a comparison was made between conditions.

A total of 5 ***network metrics*** (network density, mean nodal degree, mean nodal strength, mean clustering coefficient, and global efficiency) were computed in order to statistically compare network characteristics. Two-tailed non-parametric permutation *t*-tests with 20,000 randomizations ($P < 0.05$ Bonferroni-corrected for multiple comparisons yielding a significance threshold of $P < 0.002$) were applied to assess statistical differences. Permutation tests were chosen because they do not rely on assumptions about the underlying distribution of the measure under investigation, as this is often not known for network metrics.

The *mean nodal degree* is calculated as the average of each node's number of nonzero connections. *Mean nodal strength* describes the sum of weights of each node's connections averaged over all nodes. Both measures were normalized by division through the number of network nodes. They are measures of network integration, assessing how well the network is connected. *Global efficiency*, also a measure of network integration, was calculated as the average inverse shortest path length. Path length was defined as the sum of the inverse edge weights of all edges belonging to the path. Thereby, global efficiency assesses how well information can be propagated throughout the network. The *mean clustering coefficient* is calculated as the geometric mean of weights in triangles around a node averaged across all nodes. It can reveal the presence of functional cliques within the node's neighborhood, serving as a measure of nodal segregation.

Furthermore, the ***optimal modular decomposition*** of each network was determined by assigning nodes to modules such that the number of intra-module edges was maximized and the number of inter-module edges was minimized. This was achieved by maximizing the Newman modularity (Newman 2006) with a heuristic optimization strategy that employed the Kernighan–Lin algorithm (Sun et al. 2009). Each node was first assigned to an individual module. Then, the modularity maximization algorithm was run 100 times. Repeating the algorithm and then averaging the results reduced instability due to randomness (Fuertinger et al. 2015). As

module numbers were randomly assigned, they were then changed by means of a permutation approach to ensure maximal overlap of module assignment between groups and conditions. The *partition distance*—a measure of normalized variation of information between 2 module affiliation vectors (Meilă 2007)—was used to compare the optimal modular decompositions between groups and conditions.

In a last step of the analysis, ***hub formation*** was assessed: Any node whose nodal degree or nodal strength was >1 standard deviation (SD) above the mean was considered a hub. Highly connected nodes (nodes within top 30% of nodal degree and nodal strength) that did not meet the hub criterium were considered as high influence nodes. For further differentiation, hubs were divided into connector hubs (facilitating communication between different modules) and provincial hubs (facilitating communication within a module). For this purpose, the nodal participation coefficient (sometimes also called participation index; van den Heuvel and Sporns 2011)—a measure of the distribution of inter- vs. intra-module connections—was used, with a cut-off value of 10% of the maximum nodal participation coefficient. Hubs above the cutoff were termed connector hubs, all other hubs were classified as provincial hubs. Hubs were assessed concerning their type and spatial distribution. We then determined *network pillars*, that is, hubs which play an outstanding role in carrying the information propagation within the network. Although the concept of hubs as key network nodes is commonly used in the literature, there is no consistent definition of which nodes should be considered hubs (van den Heuvel and Sporns 2013; Oldham and Fornito 2019). We therefore decided to analyze hubs in a more detailed way. Here, we will refer to hubs whose nodal degree or nodal strength was 1.5 SD above the mean of all nodes as network pillars. The cutoff of 1.5 SD was determined in a data-driven way: all hubs were >1 SD above the mean of nodal degree or nodal strength for the respective group in the respective condition. However, no hub was >2 SD above the mean. We therefore decided to look at the hubs that where 1.5 SD above the mean in 1 of the 2 metrics. We argue that due to their exceptional number of edges and/or their exceptionally strong connections with other nodes, these hubs are especially vital for network functioning. We assessed whether pillar distribution was robust against aging and emotional distraction. The entire hub analysis is of qualitative character and reported in a descriptive manner, as it does not allow for statistical testing.

Analysis scripts were written in Python 3.7 using the aforementioned libraries. For the computation of the optimal modular decomposition and the network metrics, MATLAB (The MathWorks, Inc.) with the Brain Connectivity Toolbox (Rubinov and Sporns 2010) was employed. Furthermore, the BrainNet Viewer (Xia et al. 2013) was used for creating 3D network images within reference brain models.

Data and code availability

The data used in this study will be made available upon request under the conditions of a formal data sharing agreement. The code used for this analysis is publicly available at https://github.com/k-simonyan/NetworkAnalysis_Speech_HealthyAging.

Results

Behavioral results

There was no significant difference in speech onset between groups ($F_{1,44} = 3.02$, $P = 0.09$) nor between conditions ($F_{1,44} = 1.32$, $P = 0.26$) and there was no significant interaction effect ($F_{1,44} = 0.87$, $P = 0.36$). Participants perceived disgusted facial primes ($M = 2.49$, $SD = 0.66$) as more negative than neutral facial primes ($M = 4.96$, $SD = 0.48$; $F_{1,44} = 867.16$, $P < 0.0001$). Although elderly participants rated both neutral and disgusted pictures slightly higher than young participants, there was no significant group difference ($F_{1,44} = 1.60$, $P = 0.21$) and no significant interaction effect ($F_{1,44} = 0.51$, $P = 0.82$).

Network metrics

Using a percolation thresholding approach, the final group networks had different densities (see Table 2). However, only in the disgusted condition the young group's network was significantly denser than that of the elderly group. There was no significant condition effect on densities. Mean nodal degree and mean nodal strength differed significantly between groups. Both measures were smaller in the elderly group in both conditions. Mean nodal strength significantly differed between conditions in the young group. The mean clustering coefficient differed significantly between groups in the neutral but not in the disgusted condition. A significant condition effect was found in the young group, but not in the elderly. Global efficiency did not differ significantly between groups, but for the young group, there was a significant increase in the disgusted condition.

Communication patterns

Although the optimal modular decomposition, as measured by the partition distance, differed significantly between groups in the disgusted condition, there was no such effect in the neutral condition (see Table 3). Furthermore, there was no significant condition effect in either group. The young group had an optimal modular decomposition of 5 modules (Fig. 2): a parieto-occipital one that extended into the cerebellum (purple), a subcortical one, which extended into the cerebellum in the disgusted condition (brown), a primarily peri-central one (green), a very small module comprised of only 2 cerebellar nodes (blue), and a distributed module with nodes in frontal, parietal, and cerebellar regions (red). The elderly group had 6 modules in the neutral condition and 5 in the disgusted condition (Fig. 2). In both conditions there was an

Table 2. Network metrics for all groups and conditions.

Group		Young	Elderly	*P*
Network density	Neutral	81.04%	49.08%	0.032
	Disgusted	86.21%	49.61%	**0.0004**
	P	0.435	0.967	
Mean nodal degree	Neutral	0.81 ± 0.19	0.49 ± 0.23	**
	Disgusted	0.86 ± 0.18	0.49 ± 0.12	**
	P	0.003	0.818	
Mean nodal strength	Neutral	0.10 ± 0.03	0.07 ± 0.04	**
	Disgusted	0.11 ± 0.03	0.07 ± 0.12	**
	P	**	0.487	
Mean clustering coefficient	Neutral	0.10 ± 0.01	0.12 ± 0.02	**
	Disgusted	0.12 ± 0.02	0.12 ± 0.02	0.889
	P	**	0.044	
Global efficiency	Neutral	0.109	0.110	0.831
	Disgusted	0.125	0.113	0.046
	P	**	0.616	

**$P<0.0001$. *Note:* Mean values are given ± 1 SD. *P*-values were determined by a permutation *t*-test with 20000 repetitions. Bold font indicates statistical significance.

Table 3. Partition distances of module affiliations.

Comparison		Partition distance	*P*
Young neutral	Elderly neutral	0.252	0.057
Young disgusted	Elderly disgusted	0.307	**0.001**
Young neutral	Young disgusted	0.227	0.367
Elderly neutral	Elderly disgusted	0.132	0.497

occipital-cerebellar module (purple), a subcortical module (brown), a very small cerebellar module (blue), and a frontal module (red). In the disgusted condition, the fifth module was a parietal one (green). In the neutral condition, the parietal module was split in 2 (green and yellow).

Communication patterns differed between groups and conditions (Figs. 3 and 4). Young participants showed connector hubs in 4 different modules (2 red, 10 green, 5 purple, and 6 brown) in the neutral condition, but no connector hubs in the disgusted condition. A similar pattern was observed in the elderly group, where a smaller number of connector hubs were found in 3 modules (1 green, 5 purple, and 3 brown) in the neutral condition, but none in the disgusted condition. Young participants had fewer provincial hubs than elderly participants in both conditions. Both groups showed an increase in provincial hubs in the disgusted condition, but this increase was more pronounced in the young (young: 8 vs. 28 and elderly: 31 vs. 38). In both conditions, young participants had a higher number of high influence nodes (neutral: 61 and disgusted: 72) than elderly participants (neutral: 30 and disgusted: 23).

When looking at the network pillars (Fig. 5), nearly all pillars of the young groups' network were also pillars in the elderly groups' network. However, in the elderly groups' network, additional hubs reached pillar status. This was the case for both the neutral and the disgusted condition. In the young group, pillars were very robust against an emotional challenge. Of the 5 pillars found in the neutral condition, 4 remained in the disgusted condition (bilateral MCC and bilateral cerebellar lobule VI). Only right area 3b lost pillar status after an emotional prime. In contrast, the right temporal region of the thalamus gained pillar status.

The elderly groups' network exhibited similar pillar robustness. As with the younger group, pillars in the neutral condition remained in the disgusted condition with the sole exception of right area 3b. In addition, the right lingual gyrus and right cerebellar lobule VI gained hub status in the disgusted condition.

Discussion

In this study, we determined whole-brain functional group networks of young and elderly healthy individuals during a picture naming task and examined how healthy aging changes the SPN. We were specifically interested in the robustness of network pillars, referring to key communicative nodes in the network. By including an emotional component in our paradigm, we were also able to determine the influence of emotional priming on network characteristics in both age groups, further elucidating which network aspects remain stable after an emotional challenge.

Our analysis revealed that the SPN changes during healthy aging. We found that although the network's ability to propagate information remains stable, as determined by the fact that there is no difference in global efficiency, network segregation is indeed affected by age. In the absence of confounding factors such as emotional distraction, the clustering coefficient was increased in the elderly group, suggesting that healthy aging leads to functionally more segregated network processing. We hypothesized that our findings would reflect research on age-related effects in RSNs, which was indeed the

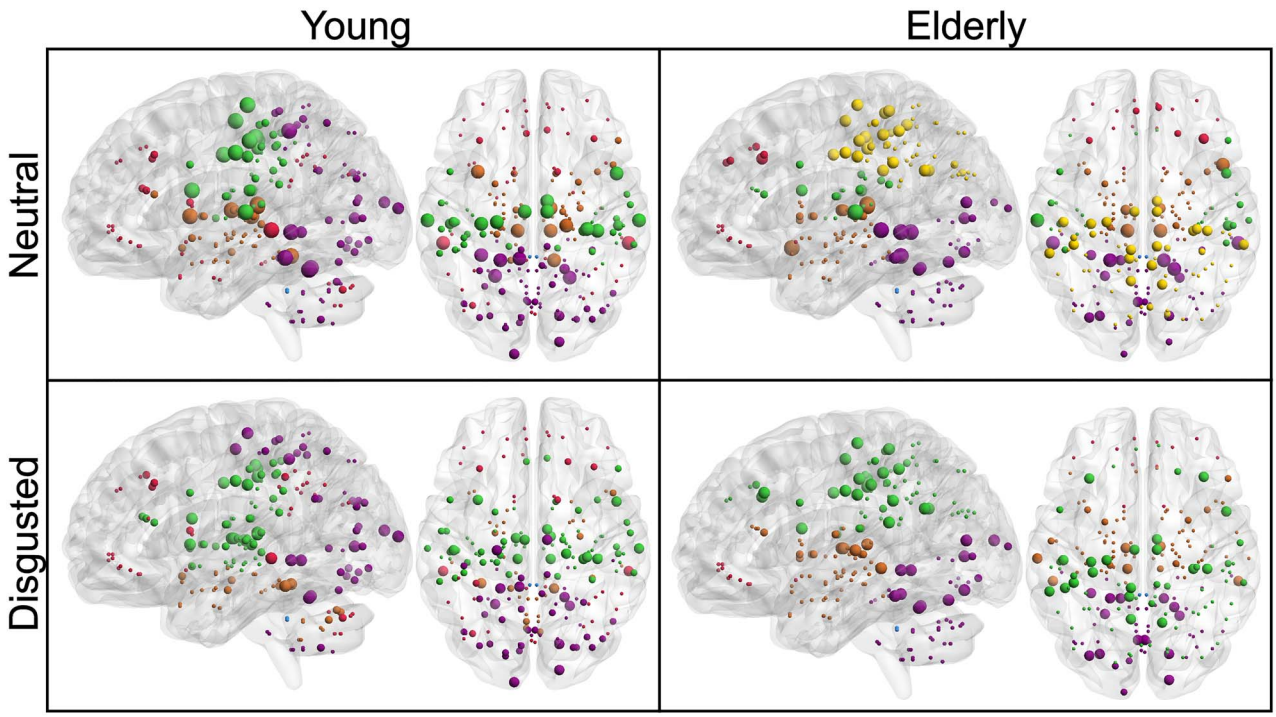

Fig. 2. Optimal modular decomposition and hub localization for each group and condition. Module affiliation is indicated by color: purple—parietal-occipital-cerebellar module; brown—subcortical module; blue—cerebellar module; red—frontal module; green and yellow—parietal modules. Hub characteristics are denoted by size: Largest nodes indicate connector hubs, followed by provincial hubs, high influence nodes and other nodes. Although the optimal modular decomposition does not differ much between groups or conditions, hub characteristics and localization vary.

case. The RSN has been shown to exhibit stable network integration (Song et al. 2014; Geerligs et al. 2015; Varangis et al. 2019) and increasing network segregation as measured by the clustering coefficient (Sala-Llonch et al. 2014; Shah et al. 2018) during aging. However, contradicting studies on network segregation have reported a decrease in measures of segregation other than the clustering coefficient (Chan et al. 2014; Song et al. 2014).

We also hypothesized that age influences SPN communication patterns. Our qualitative hub analysis showed that healthy aging was associated with the presence of fewer connector hubs and more provincial hubs, indicating that speech processing was achieved in a more modularized manner than in young individuals. This fits with our finding that the older network was more functionally segregated. Although the optimal modular decomposition did not differ significantly between groups in the neutral condition, which has previously also been shown for resting state data (Meunier et al. 2009), the interplay of the modules changed with age. Meunier et al. (2009) report a shift in communication patterns similar to what we found. The number of network modules they determined for each group (5 for young individuals and 6 for older individuals) are the same that we observed, and their spatial distribution is very similar as well. This underlines our idea that aging effects on the SPN reflect those on the RSN.

Our analysis of network pillars, that is, nodes carrying the communicative load of the network, revealed that areas, which are especially strong communicators within the young network are robust against aging and do not lose their pillar status. On the contrary, aging leads to an increase in the number of such pillars. In the young group, the MCC and the cerebellum, both bilaterally, and reached pillar status. The MCC has been reported to play a pivotal role in social cognition and the integration of emotional processing and motor signals (Pereira et al. 2010; Apps et al. 2013). Furthermore, it is known to be functionally connected to premotor, frontal, parietal, and subcortical areas (Hoffstaedter et al. 2014), supporting its status as a network pillar. The cerebellum has been implicated to play a role in emotion perception and word retrieval (De Smet et al. 2013; Adamaszek et al. 2017), both of which were crucial aspects in the task at hand.

In the elderly individuals' network, more regions reached pillar status. Bilateral MCC and cerebellum were again found to be network pillars, underlining their importance for the speech production network. In addition to these regions, which retained their pillar status during healthy aging, the left fusiform gyrus, the left lingual gyrus, and the left medial temporal gyrus were new network pillars. Although the fusiform gyrus is widely known for its role in face perception, it is also implicated in object recognition (Weiner and Zilles 2016). The lingual gyrus has been found to play a role in the processing of facial expressions (Kesler-West et al. 2001; Kitada et al. 2010). Although the function of the medial temporal gyrus is very diverse, it seems to be active during facial and language processing (Xu et al. 2015). We conclude that the elderly's network distributed the

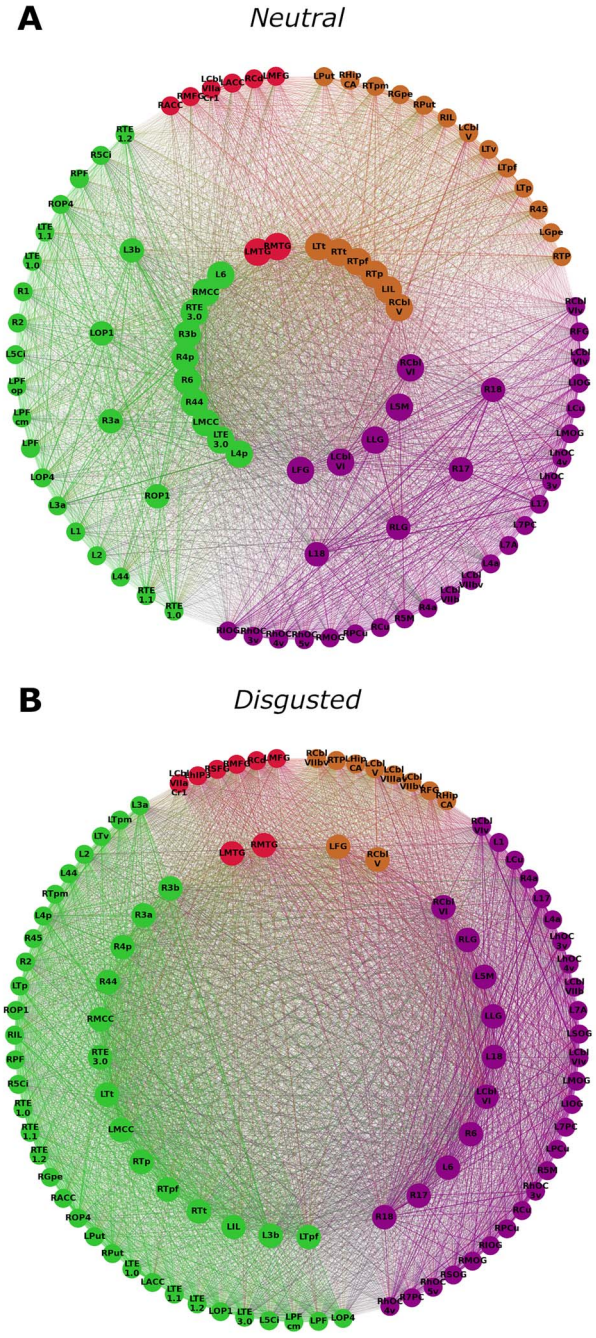

Fig. 3. Hub characteristics of the young group's networks. Only nodes that are hubs or high influence nodes are being displayed. Nodes are arranged in 3 circles. Connector hubs are placed on the inner circle, provincial hubs on the intermediate circle and high influence nodes on the outer circle. Colors indicate module affiliation: purple—parietal-occipital-cerebellar module; brown—subcortical module; red—frontal module; green—parietal module (see Fig. 2). Young participants exhibit connector hubs in the neutral condition but not in the disgusted condition. However, in the disgusted condition the number of provincial hubs is greater than in the neutral condition.

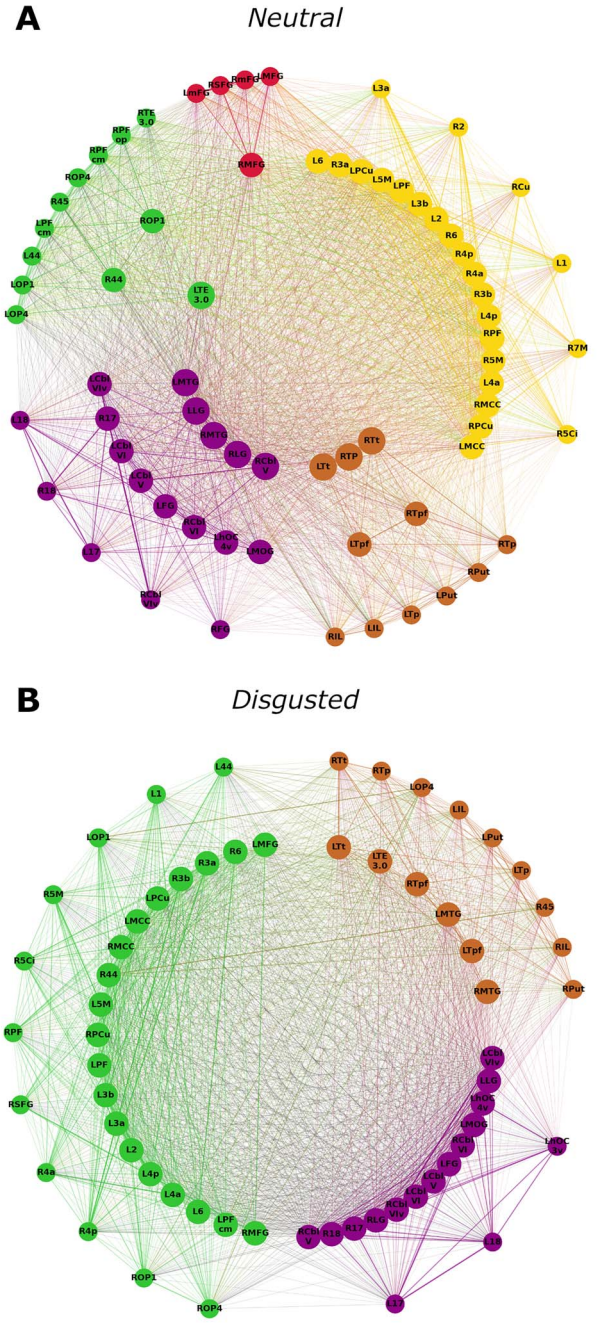

Fig. 4. Hub characteristics of the elderly group's networks. Only nodes that are hubs or high influence nodes are being displayed. Nodes are arranged in 3 circles. Connector hubs are placed on the inner circle, provincial hubs on the intermediate circle and high influence nodes on the outer circle. Colors indicate module affiliation: purple—occipital-cerebellar module; brown—subcortical module; red—frontal module; green and yellow—parietal modules (see Fig. 2). Elderly participants exhibit connector hubs in the neutral condition but not in the disgusted condition. In the disgusted condition the number of provincial hubs is greater than in the neutral condition. Furthermore, in the neutral condition hubs are distributed over 5 modules, whereas in the disgusted condition they only appear in 3 modules.

communicative load between more task-relevant regions than the young group's network. This might be one processing strategy to ensure successful functioning in the presence of the reported age-related network changes.

The secondary aim of our study was to investigate how emotional priming influences the SPN and whether these influences change during healthy aging. Our behavioral analysis revealed that disgusted facial primes were

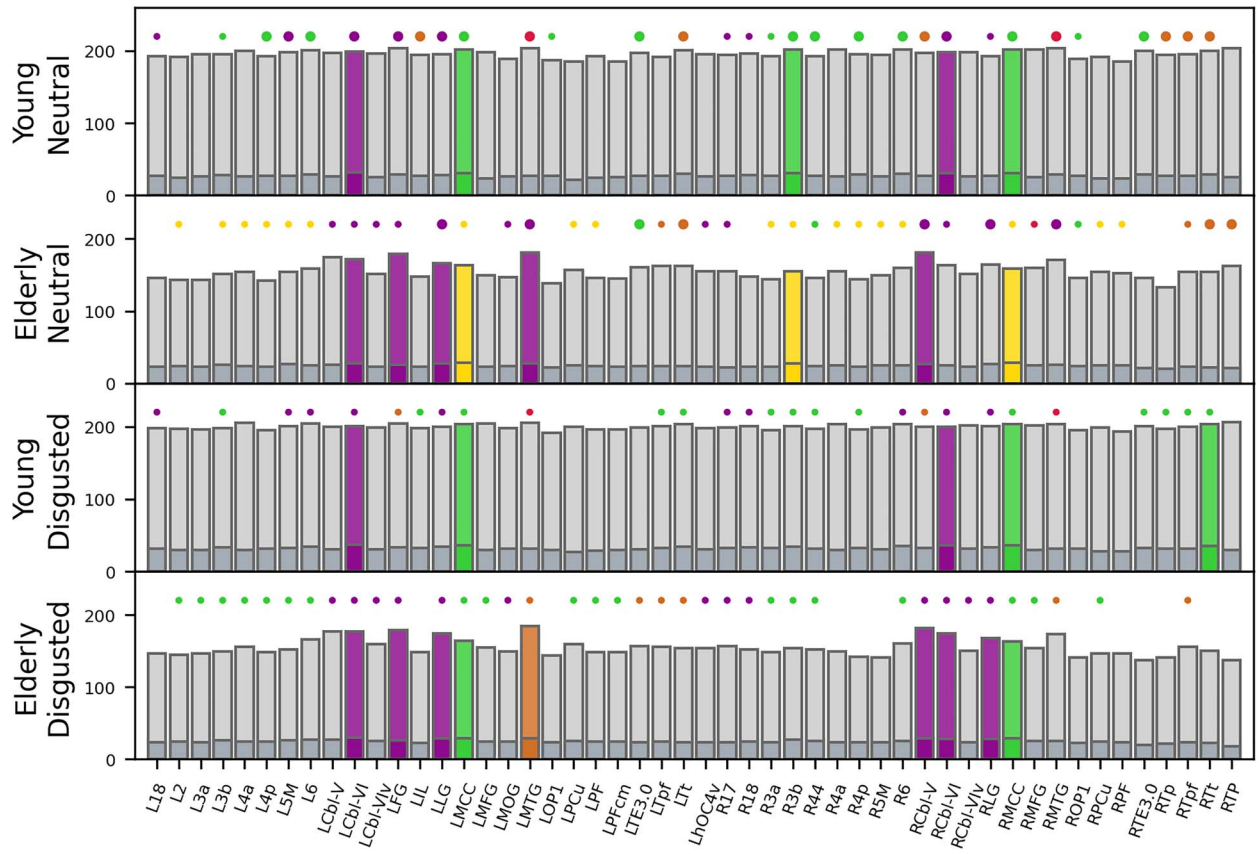

Fig. 5. Network pillars. Bars depict nodal degree (light gray) and nodal strength (dark gray) for all hub nodes. Large circles denote connector hubs, smaller circles denote provincial hub. The absence of a circle means that this node was not a hub in the respective network. Color indicates module affiliation. Colored bars depict network pillars. *Abbreviations*: R, right; L, left; 2/3a/3b/6/17/18/44, Brodmann areas (BA) 2/3a/3b/6/17/18/44; 4a/4p, anterior/posterior part of BA 4; 5M, subdivision of BA 5; Cbl-V/VI/VIv, cerebellar lobules V/VI/VI vermis; FG, fusiform gyrus; hOC4v, ventral part of area hOC4; IL, insula; LG, lingual gyrus; MCC, middle cingulate cortex; MFG, middle frontal gyrus; MOG, middle occipital gyrus; MTG, middle temporal gyrus; OP1, operculum; PCu, precuneus; PF/PFcm, area PF/PFcm in the inferior parietal cortex; TE3.0, area TE3.0 in the auditory cortex; Tp/Tpf/Tt, parietal/prefrontal/temporal subdivisions of the thalamus; and TP, temporal pole.

indeed perceived as being more negative than neutral facial primes, solidifying our paradigm. We were able to show that priming the picture naming task with a negative emotional stimulus (a disgusted face) lead to distinct network changes in the young group. Mean nodal strength and mean clustering coefficient, as well as global efficiency increased during emotional processing. There also was a trend for mean nodal degree, but this did not remain after Bonferroni correction. We further found that network communication patterns shifted from primarily intermodular connections (many connector hubs and few provincial hubs) to predominantly intramodular communication, where no connector hubs were present at all. This indicates more segregated network function. To our knowledge, there is no literature on neutral vs. disgusted priming effects on whole-brain functional connectivity, but a study on affective processing by Zhang et al. (2015) found that affective functional networks are more segregated than neutral networks, supporting our findings (note that Zhang et al. (2015) report less integrated affective networks, whereas we found an increase in 2 measures of network integration). One possible explanation for increased segregation could be that when faced with potentially dangerous stimuli, communication between network modules is downregulated to prioritize fast intramodular processing. However, the design of the current study does not allow verification of this assumption.

We were able to show that emotional priming effects are less pronounced in the elderly group's network, as hypothesized. The only network metric affected by priming was the clustering coefficient, and the observed increase in this metric was much smaller than in the young group. In terms of communication patterns, we found the same qualitative changes as seen in the young group (loss of connector hubs and increase of provincial hubs), but also in this case the changes were less pronounced than in the young group. We suggest that our findings illustrate neural correlates of an increased robustness against emotional distraction in healthy aging. Our study therefore provides a network explanation for the positivity effect (Carstensen and Mikels 2005; Nashiro et al. 2012; Kehoe et al. 2013; Ge et al. 2014) and the finding that emotional regulation

improves over the life span (Mather and Carstensen 2005; Mather and Knight 2005; Eldesouky and English 2018).

When looking at network pillars, we found that they remain stable after emotional distraction. In the young group, the number of network pillars was the same in both conditions. The elderly's network exhibited one pillar more in the disgusted condition than in the neutral one. We argue that network pillars represent key communicative players within networks, which are stable against aging and emotional challenge.

It should be noted that the current analysis does not provide information as to when the reported network changes occur. As the study was cross-sectional and did not include groups of intermediate age steps, it remains unclear whether these network changes occur progressively during adult life or whether there is a certain point at which changes start to manifest. The mean age of the young group was ~24 years. Studies on synaptic circuitry have reported that the period for developmental changes extends into the third decade of life, and that these changes underlie dynamic reorganization of the synaptic circuitry (Petanjek et al. 2011). It is therefore possible that the network changes observed here reflect these developmental changes to some extent. Further analyses stratifying different periods of life would be necessary to discern when network alterations occur.

Applying both GLM (Supplementary Figs. S1 and S2, Table S1) and graph-theoretical analysis methods to the same data set enabled us to highlight that these methods can show complementary results. The GLM analysis showed that the regions involved in solving the task were very similar between groups and conditions. Especially the condition contrasts revealed no difference in activation patterns. GLM analysis is therefore not sufficient to illustrate how the conditions differ concerning brain activity. Only by also looking at the graph-theoretical results one can see a difference between the processing of neutral vs. emotionally loaded tasks. The graph-theoretical analysis revealed profound differences in the processing of the 2 conditions.

Although our study provides new insight into network changes underlying age-related speech production alterations, one should consider its limitations. First, there is no literature yet on appropriate sample sizes for fMRI network analyses. Our sample size of 23 participants per group might therefore not be sufficient to reflect real population effects. However, our sample size is similar to that of many studies in this field (Meunier et al. 2009; Song et al. 2014; Fuertinger et al. 2015; Simonyan and Fuertinger 2015; Fuertinger and Simonyan 2017). Furthermore, our results are in line with studies reporting much larger sample sizes (Geerligs et al. 2015; Shah et al. 2018; Varangis et al. 2019). A second limitation is the rather complex task design combining visual and speech-related motor elements. Picture naming was chosen as a well-established paradigm involving all levels of language production. However, it does not only yield language-related activation, but also visual activation. Furthermore, by adding an emotional aspect into the paradigm, it became even more complex. We believe that the benefits of using this paradigm outweigh the difficulties arising regarding its interpretability, as it yielded results comparable with those of other studies and gave new insight into network function, especially concerning the location and stability of network pillars.

Conclusion

We investigated the effects of healthy aging and emotional priming on the speech production network. We were able to show aging effects on the SPN reflect those on the RSN, and that SPN in the elderly is more robust against emotional priming than that in the young. Our study provides a network perspective on the positivity effect (Carstensen and Mikels 2005) and the elderly's increased capacity for emotional regulation (Eldesouky and English 2018). Furthermore, we identified pillars mostly localized in tertiary associative areas of the cortex representing key communicative players within networks, which are stable against aging and emotional challenges.

Acknowledgments

The authors would like to thank Peter Sörös for his help in data curation as well as his valuable input concerning data analysis and interpretation.

Supplementary material

Supplementary material is available at *Cerebral Cortex* online.

Funding

This work was supported by the National Institutes of Health (R01NS088160, R01DC011805, and R01DC012545 to KS); the Department of Defense (W911NF1810434 to KS); Amazon Web Services to KS; and Mass General Brigham Innovation to KS.

Conflict of interest statement. KS serves on the Scientific Advisory Board of the Tourette Association of America. JS, CM, MC, CT, and KW report no conflicts of interest.

References

Abrams L, Farrell MT. Language processing in normal aging. *The handbook of psycholinguistic and cognitive processes: perspectives in communication disorders*. New York, NY, US: Psychology Press; 2011. pp. 49–73

Adamaszek M, D'Agata F, Ferrucci R, Habas C, Keulen S, Kirkby K, Leggio M, Mariën P, Molinari M, Moulton E. Consensus paper: cerebellum and emotion. *Cerebellum*. 2017:16:552–576.

Apps MA, Lockwood PL, Balsters JH. The role of the midcingulate cortex in monitoring others' decisions. *Front Neurosci*. 2013:7:251.

Avants BB, Tustison NJ, Song G, Cook PA, Klein A, Gee JC. A reproducible evaluation of ANTs similarity metric performance in brain image registration. *NeuroImage*. 2011:54:2033–2044.

Beck AT, Steer RA, Brown G. Beck depression inventory–II. San Antonio, TX: Psychological Corporation. 1996.

Blank SC, Scott SK, Murphy K, Warburton E, Wise RJS. Speech production: Wernicke, Broca and beyond. *Brain*. 2002:125:1829–1838.

Bordier C, Nicolini C, Bifone A. Graph analysis and modularity of brain functional connectivity networks: searching for the optimal threshold. *Front Neurosci*. 2017:11:441.

Brodeur MB, Guérard K, Bouras M. Bank of standardized stimuli (BOSS) phase II: 930 new normative photos. *PLoS One*. 2014:9:e106953.

Bullmore E, Sporns O. Complex brain networks: graph theoretical analysis of structural and functional systems. *Nat Rev Neurosci*. 2009:10:186–198.

Carstensen LL, Mikels JA. At the intersection of emotion and cognition: aging and the positivity effect. *Curr Dir Psychol Sci*. 2005:14:117–121.

Chan MY, Park DC, Savalia NK, Petersen SE, Wig GS. Decreased segregation of brain systems across the healthy adult lifespan. *Proc Natl Acad Sci*. 2014:111:E4997–E5006.

Cole MW, Bassett Danielle S, Power Jonathan D, Braver Todd S, Petersen SE. Intrinsic and task-evoked network architectures of the human brain. *Neuron*. 2014:83:238–251.

Cole MW, Ito T, Bassett DS, Schultz DH. Activity flow over resting-state networks shapes cognitive task activations. *Nat Neurosci*. 2016:19:1718–1726.

Cover TM, Thomas JA. *Elements of information theory*. New York: John Wiley & Sons; 2012.

Cox RW. AFNI: software for analysis and visualization of functional magnetic resonance neuroimages. *Comput Biomed Res*. 1996:29:162–173.

Dagerman KS, MacDonald MC, Harm MW. Aging and the use of context in ambiguity resolution: complex changes from simple slowing. *Cogn Sci*. 2006:30:311–345.

De Smet HJ, Paquier P, Verhoeven J, Mariën P. The cerebellum: its role in language and related cognitive and affective functions. *Brain Lang*. 2013:127:334–342.

Di X, Gohel S, Kim EH, Biswal BB. Task vs. rest-different network configurations between the coactivation and the resting-state brain networks. *Front Hum Neurosci*. 2013:7:493.

Dolcos F, McCarthy G. Brain systems mediating cognitive interference by emotional distraction. *J Neurosci*. 2006:26:2072–2079.

Eickhoff SB, Stephan KE, Mohlberg H, Grefkes C, Fink GR, Amunts K, Zilles K. A new SPM toolbox for combining probabilistic cytoarchitectonic maps and functional imaging data. *NeuroImage*. 2005:25:1325–1335.

Eldesouky L, English T. Another year older, another year wiser? Emotion regulation strategy selection and flexibility across adulthood. *Psychol Aging*. 2018:33:572–585.

Friston KJ. Functional and effective connectivity: a review. *Brain Connect*. 2011:1:13–36.

Fuertinger S, Simonyan K. Connectome-wide phenotypical and genotypical associations in focal dystonia. *J Neurosci*. 2017:37:7438–7449.

Fuertinger S, Horwitz B, Simonyan K. The functional connectome of speech control. *PLoS Biol*. 2015:13:e1002209.

Ge R, Fu Y, Wang D, Yao L, Long Z. Age-related alterations of brain network underlying the retrieval of emotional autobiographical memories: an fMRI study using independent component analysis. *Front Hum Neurosci*. 2014:8:629.

Geerligs L, Renken RJ, Saliasi E, Maurits NM, Lorist MM. A brain-wide study of age-related changes in functional connectivity. *Cereb Cortex*. 2015:25:1987–1999.

Gupta R, Raymond JE. Emotional distraction unbalances visual processing. *Psychon Bull Rev*. 2012:19:184–189.

Heim S. The structure and dynamics of normal language processing: insights from neuroimaging. *Acta Neurobiol Exp (Wars)*. 2005:65:95–116.

Hickok G, Poeppel D. The cortical organization of speech processing. *Nat Rev Neurosci*. 2007:8:393–402.

Hoffstaedter F, Grefkes C, Caspers S, Roski C, Palomero-Gallagher N, Laird AR, Fox PT, Eickhoff SB. The role of anterior midcingulate cortex in cognitive motor control: evidence from functional connectivity analyses. *Hum Brain Mapp*. 2014:35:2741–2753.

Humphries MD, Gurney K, Prescott TJ. The brainstem reticular formation is a small-world, not scale-free, network. *Proc Biol Sci*. 2006:273:503–511.

Hunter JD. Matplotlib: a 2D graphics environment. *Comput Sci Eng*. 2007:9:90–95.

Hur J, Iordan AD, Dolcos F, Berenbaum H. Emotional influences on perception and working memory. *Cognit Emot*. 2017:31:1294–1302.

Kehoe EG, Toomey JM, Balsters JH, Bokde AL. Healthy aging is associated with increased neural processing of positive valence but attenuated processing of emotional arousal: an fMRI study. *Neurobiol Aging*. 2013:34:809–821.

Kesler-West ML, Andersen AH, Smith CD, Avison MJ, Davis CE, Kryscio RJ, Blonder LX. Neural substrates of facial emotion processing using fMRI. *Cogn Brain Res*. 2001:11:213–226.

Kitada R, Johnsrude IS, Kochiyama T, Lederman SJ. Brain networks involved in haptic and visual identification of facial expressions of emotion: an fMRI study. *NeuroImage*. 2010:49:1677–1689.

Langner O, Dotsch R, Bijlstra G, Wigboldus DHJ, Hawk ST, van Knippenberg A. *Presentation and validation of the Radboud Faces Database*. United Kingdom: Taylor & Francis; 2010. pp. 1377–1388

Lustig C, Hasher L, Zacks RT. *Inhibitory deficit theory: recent developments in a" new view"*. Inhibition in cognition. 2007:145–162.

Lynall ME, Bassett DS, Kerwin R, McKenna PJ, Kitzbichler M, Muller U, Bullmore E. Functional connectivity and brain networks in schizophrenia. *J Neurosci*. 2010:30:9477–9487.

MacDonald MC, Christiansen MH. *Reassessing working memory: comment on Just and Carpenter (1992) and Waters and Caplan (1996)*. Psychological Review, 2002:109:35–54.

MacKay DG, Burke DM. Cognition and aging: a theory of new learning and the use of old connections. In: T. M. Hess (Ed.), *Aging and cognition: knowledge organization and utilization*. North-Holland. 1990. p. 213–263.

Mather M, Carstensen LL. Aging and motivated cognition: the positivity effect in attention and memory. *Trends Cogn Sci*. 2005:9:496–502.

Mather M, Knight M. Goal-directed memory: the role of cognitive control in older adults' emotional memory. *Psychol Aging*. 2005:20:554.

Meilă M. Comparing clusterings—an information based distance. *J Multivar Anal*. 2007:98:873–895.

Meunier D, Achard S, Morcom A, Bullmore E. Age-related changes in modular organization of human brain functional networks. *NeuroImage*. 2009:44:715–723.

Mortensen L, Meyer AS, Humphreys GW. Age-related effects on speech production: a review. *Lang Cogn Process*. 2006:21:238–290.

Nashiro K, Sakaki M, Mather M. Age differences in brain activity during emotion processing: reflections of age-related decline or increased emotion regulation. *Gerontology*. 2012:58:156–163.

Newman ME. Modularity and community structure in networks. *Proc Natl Acad Sci*. 2006:103:8577–8582.

Oldham S, Fornito A. The development of brain network hubs. *Dev Cogn Neurosci*. 2019:36:100607.

Oliphant TE. *Guide to NumPy: create space independent publishing platform*. Austin, TX. 2015.

Pereira MG, de Oliveira L, Erthal FS, Joffily M, Mocaiber IF, Volchan E, Pessoa L. Emotion affects action: midcingulate cortex as a pivotal node of interaction between negative emotion and motor signals. *Cogn Affect Behav Neurosci*. 2010:10:94–106.

Petanjek Z, Judaš M, Šimić G, Rašin MR, Uylings HB, Rakic P, Kostović I. Extraordinary neoteny of synaptic spines in the human prefrontal cortex. *Proc Natl Acad Sci*. 2011:108:13281–13286.

Price CJ. A review and synthesis of the first 20years of PET and fMRI studies of heard speech, spoken language and reading. *NeuroImage*. 2012:62:816–847.

Roux F, Armstrong BC, Carreiras M. Chronset: an automated tool for detecting speech onset. *Behav Res Methods*. 2017:49:1864–1881.

Rubinov M, Sporns O. Complex network measures of brain connectivity: uses and interpretations. *NeuroImage*. 2010:52: 1059–1069.

Sala-Llonch R, Junqué C, Arenaza-Urquijo EM, Vidal-Piñeiro D, Valls-Pedret C, Palacios EM, Domènech S, Salvà A, Bargalló N, Bartrés-Faz D. Changes in whole-brain functional networks and memory performance in aging. *Neurobiol Aging*. 2014:35: 2193–2202.

Shah C, Liu J, Lv P, Sun H, Xiao Y, Liu J, Zhao Y, Zhang W, Yao L, Gong Q, et al. Age related changes in topological properties of brain functional network and structural connectivity. *Front Neurosci*. 2018:12:318–318.

Shannon CE. A mathematical theory of communication. *Bell Syst Tech J*. 1948:27:379–423.

Simonyan K, Fuertinger S. Speech networks at rest and in action: interactions between functional brain networks controlling speech production. *J Neurophysiol*. 2015:113:2967–2978.

Song J, Birn RM, Boly M, Meier TB, Nair VA, Meyerand ME, Prabhakaran V. Age-related reorganizational changes in modularity and functional connectivity of human brain networks. *Brain Connect*. 2014:4:662–676.

Sörös P, Sokoloff LG, Bose A, McIntosh AR, Graham SJ, Stuss DT. Clustered functional MRI of overt speech production. *NeuroImage*. 2006:32:376–387.

Sörös P, Bose A, Sokoloff LG, Graham SJ, Stuss DT. Age-related changes in the functional neuroanatomy of overt speech production. *Neurobiol Aging*. 2011:32:1505–1513.

Sun Y, Danila B, Josić K, Bassler KE. Improved community structure detection using a modified fine-tuning strategy. *EPL (Europhysics Letters)*. 2009:86:28004.

Tukey JW. *Exploratory data analysis*. Reading, Mass: Addison-Wesley Pub. Co. 1977.

van den Heuvel MP, Sporns O. Rich-club organization of the human connectome. *J Neurosci*. 2011:31:15775–15786.

van den Heuvel MP, Sporns O. Network hubs in the human brain. *Trends Cogn Sci*. 2013:17:683–696.

Varangis E, Habeck C, Razlighi Q, Stern Y. The effect of aging on resting state connectivity of predefined networks in the brain. *Front Aging Neurosci*. 2019:11:234.

Veale JF. Edinburgh handedness inventory – short form: a revised version based on confirmatory factor analysis. *Laterality*. 2014:19: 164–177.

Virtanen P, Gommers R, Oliphant TE, Haberland M, Reddy T, Cournapeau D, Burovski E, Peterson P, Weckesser W, Bright J. SciPy 1.0: fundamental algorithms for scientific computing in Python. *Nat Methods*. 2020:1-12.

Weiner KS, Zilles K. The anatomical and functional specialization of the fusiform gyrus. *Neuropsychologia*. 2016:83:48–62.

Xia M, Wang J, He Y. BrainNet viewer: a network visualization tool for human brain connectomics. *PLoS One*. 2013:8.

Xu J, Wang J, Fan L, Li H, Zhang W, Hu Q, Jiang T. Tractography-based parcellation of the human middle temporal gyrus. *Sci Rep*. 2015:5:18883.

Zhang W, Li H, Pan X. Positive and negative affective processing exhibit dissociable functional hubs during the viewing of affective pictures. *Hum Brain Mapp*. 2015:36:415–426.